Multiscale Multispectral–Hyperspectral Data for Estimating Coffee Yield Using Machine Learning Algorithms

George Deroco Martins[1], Lucas Henrique Vicentini Viana de Carvalho[1], Filipe Vieira da Silva[1], Rayssa Santos Barbosa[1], Maria Cecília Lemes Santos[1]

[1]Federal University of Uberlândia (UFU), Uberlândia, Minas Gerais, Brazil – (deroco, vicentini, lipesilva, rayssabsantos, Maria.lemes)@ufu.br

Keywords: Coffee; Hyperspectral and Multispectral; Yield Estimation; Neural Networks; Remote Sensing.

Abstract

This study evaluated the performance of multispectral (Mavic 3M) and hyperspectral (Blue Wave) data in estimating coffee crop productivity using linear regression, SVM, and neural networks. Forty plots with different varieties were analyzed. Multispectral data showed high correlation with productivity, especially the Red Edge (r = 0.704) and Green (r = 0.644) bands. For hyperspectral data, PRI (r = 0.535), GNDVI (r = -0.394), NDVI (r = -0.33), and CIRE (r = -0.328) were significant, highlighting the negative correlation pattern typically observed in perennial crops. Neural network models applied to hyperspectral data achieved the best performance (r = 0.92; RMSE = 6.6%), surpassing multispectral models (r = 0.84; RMSE = 9.4%).

1. Introduction

Estimating coffee crop productivity remains one of the major challenges in precision agriculture, particularly because this metric is only available after harvest and exhibits high variability among plants and field zones. Traditionally, this estimate is performed manually or extrapolated from harvested samples, making the process labor-intensive, time-consuming, and imprecise for large areas (Rosas et al., 2022). Considering the global economic relevance of *Coffea arabica*—responsible for more than 60% of world coffee production and the livelihood of millions of farmers in tropical regions—the development of rapid, accurate, and spatially explicit techniques for yield estimation is an urgent need (ICO, 2023; FAO, 2024).

Although traditional approaches still prevail, field visual estimates remain widely adopted by coffee growers, particularly for harvest planning. However, these methods are subjective, dependent on the observer's experience, and unable to provide a comprehensive spatial overview of the plantation. In this scenario, multispectral imagery from unmanned aerial vehicles (UAVs) emerges as a promising alternative, enabling the acquisition of high-resolution spatial data capable of detecting vigor variations associated with productivity (Sun et al., 2022). This approach allows flexible data collection across different phenological stages, supporting site-specific management and resource optimization (Singh et al., 2020).

To ensure the reliability of UAV-based data, well-defined acquisition protocols are essential, including flight altitude, drone speed, image acquisition timing, and selected spectral bands. These parameters directly affect reflectance quality and, consequently, the accuracy of vegetation indices and predictive models (Zhou et al., 2025).

Despite technological advances, standardized protocols for field radiometric data acquisition in coffee plantations are still lacking. Factors such as sensor position, canopy shading, and plant architecture introduce significant variability in reflectance readings. Unlike annual crops with homogeneous canopies, coffee plants exhibit complex and irregular structures, making multiscale radiometric calibration an additional challenge (Martins et al., 2023).

In this context, hyperspectral remote sensing arises as a complementary and powerful tool, given its fine spectral resolution that enables the detection of subtle physiological and biochemical differences in vegetation (Joshi et al., 2023). Compared with multispectral sensors, hyperspectral systems provide hundreds of contiguous bands, allowing better discrimination of chlorophyll, biomass, and water absorption features (Khan et al., 2022). Despite their higher operational complexity and cost, hyperspectral sensors offer valuable information about crop nutritional status and stress conditions—factors closely linked to yield potential (Sahoo et al., 2024).

The integration of multispectral and hyperspectral data therefore represents a promising strategy for understanding canopy functioning at multiple scales, balancing spectral detail with spatial coverage. This combination allows linking field-level variability to plant physiological responses, strengthening the use of remote sensing as an operational tool for yield estimation.

In this sense, several vegetation indices derived from reflectance measurements have been extensively used to monitor crop growth and productivity. Indices such as NDVI, GNDVI, NDRE, and PRI quantify physiological and structural canopy attributes, correlating with chlorophyll concentration, biomass, and photosynthetic efficiency (Xue & Su, 2017; Radočaj et al., 2023). In coffee plantations, these indices can reveal spatial patterns of vigor and fruit load (Rosas et al., 2022; Sun et al., 2022). However, interpreting these indices requires caution, since high vegetative vigor does not always correspond to higher productivity, especially during fruiting stages when resources are redirected from leaves to berries.

Meanwhile, the evolution of artificial intelligence algorithms has expanded the ability to model complex relationships between spectral variables and agronomic attributes. Models such as support vector machines, artificial neural networks, and linear regressions have been successfully applied to yield prediction, including in perennial crops characterized by high spatial variability (Upadhyay et al., 2025). These algorithms effectively handle multicollinearity among spectral variables and capture nonlinear relationships often missed by traditional statistical methods.

This contribution has been peer-reviewed. The double-blind peer-review was conducted on the basis of the full paper.
https://doi.org/10.5194/isprs-annals-XI-3-2026-757-2026

Integrating such models with multiscale spectral data enhances predictive capacity and supports the development of operational monitoring systems. For *Coffea arabica*, the most suitable period for yield estimation based on imagery is near harvest, when fruit load is already defined and strongly influences the plant’s spectral response. Rapid assessments at this stage enable the identification of more and less productive field zones, optimizing harvest logistics and management strategies (Martins et al., 2023).

Thus, combining UAV-based multispectral imagery with ground-based hyperspectral measurements represents a robust methodological alternative for more accurate yield estimation (Lu et al., 2019; Singh et al., 2020). This study hypothesizes that radiometric data acquired at different scales—multispectral aerial images and ground hyperspectral curves—can estimate coffee productivity with satisfactory accuracy when integrated with machine learning models and standardized acquisition protocols. The objective was to test this hypothesis by correlating spectral variables with fresh fruit weight per plot, using predictive models based on image-derived and hyperspectral attributes.

2. Material and methods

2.1 Study Area

The experiment was conducted at the Federal University of Uberlândia, Monte Carmelo Campus, located in the Triângulo Mineiro and Alto Paranaíba mesoregion, Minas Gerais, Brazil (18°43′41″ S, 47°31′26″ W, 903 m altitude). The region presents a tropical climate (Aw type, Köppen classification), characterized by a well-defined dry season from May to September and an average annual rainfall of approximately 1,600 mm.

The coffee plantation was established in December 2016, with a spacing of 3.5 m between rows and 0.6 m between plants. Five blocks were selected, totaling 39 plots with 10 plants each (Figure 1), to evaluate the Coffea arabica cultivar Topázio MG-1190 (Figure 2). This layout ensured spatial representativeness and minimized potential effects of soil heterogeneity and management variability across the experimental area.

Productivity data were obtained by harvesting fresh fruits from each plot and determining the total fruit weight per 10 plants, expressed in kilograms per plot. Statistical analysis of productivity revealed a mean value of 12.36 kg per plot, with a standard deviation of 5.44 kg and variance of 29.61. The minimum and maximum yields were 2.5 kg and 20.0 kg, respectively, indicating moderate variability among plots. The first quartile, median, and third quartile were 8.0 kg, 12.0 kg, and 18.0 kg, respectively. The distribution was approximately normal, as confirmed by the Anderson–Darling normality test ($A^2 = 0.32$; $p = 0.511$), with slight negative skewness (–0.28) and flattened kurtosis (–0.59). The 95% confidence interval for the mean ranged from 9.75 to 14.99 kg, and for the median from 8.86 to 15.41 kg.

These results indicate a moderate degree of heterogeneity within the experimental area, reflecting natural variations in plant vigor, fruit load, and microenvironmental conditions. The confirmation of normality supports the use of parametric statistical models in subsequent correlation and regression analyses.

Figure 1. Distribution and location of coffee plants evaluated.

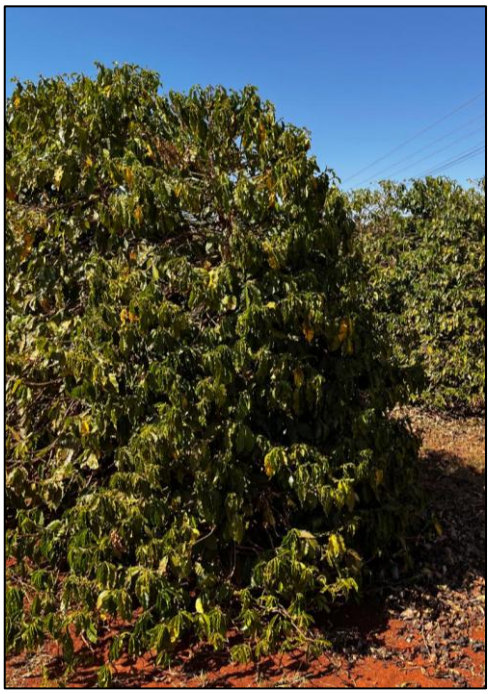

Figure 2. Coffee plant of the cultivar Topázio MG-1190.

2.2 Methodological Workflow

The methodological workflow was designed to integrate multispectral and hyperspectral data for coffee phenotyping and productivity modeling (Figure 3).

This structure ensured consistency between field and aerial data, allowing cross-scale analysis of spectral information. Data collection was conducted under similar environmental and illumination conditions to minimize the influence of external factors such as solar angle or cloud cover (Singh et al., 2020).

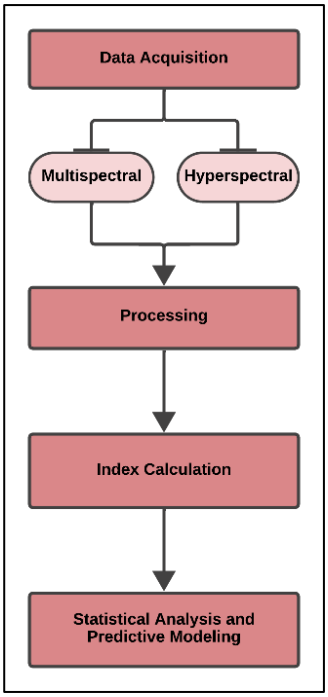

Figure 3. Methodological flowchart.

2.3 Data Acquisition

2.3.1 Multispectral: Multispectral data were acquired before harvest (June 2025) using a DJI Mavic 3M UAV (Figure 4), equipped with a multispectral sensor containing four narrow bands—Green (~560 nm), Red (~650 nm), Red Edge (~730 nm), and Near-Infrared (~840 nm). The flight was conducted at a 30 m altitude, resulting in a ground sampling distance (GSD) of approximately 2 cm/pixel. The flight plan was configured in DJI Pilot 2, with 80% forward and 75% side overlap to ensure sufficient image redundancy for accurate photogrammetric reconstruction.


Figure 4. The DJI Mavic 3M UAV.

All images were captured near solar noon (11:30–12:30 local time) under clear-sky conditions, minimizing shadowing and bidirectional reflectance distortions. The UAV’s RTK module ensured centimeter-level geolocation accuracy. A set of calibrated reflectance panels (10%, 50%, and 99%) was photographed before and after the flight to support external radiometric correction (Aasen et al., 2018).

Although the Mavic 3M sensor internally provides reflectance-calibrated imagery using an integrated Lambertian reference panel, DJI does not disclose details about the internal radiometric algorithms. Therefore, an external empirical correction was applied to validate and adjust reflectance values derived from the UAV. This approach reduced potential uncertainties caused by proprietary onboard corrections and environmental illumination differences, ensuring data reliability and inter-sensor comparability (Martins et al., 2023).

2.3.2 Hyperspectral: Hyperspectral measurements were collected on the same day using a Blue Wave spectroradiometer - StellarNet Inc. (Figure 5), covering the 350–1,000 nm spectral range with a 1.5 nm spectral resolution. The sensor was positioned 30 cm above the coffee canopy in a nadir orientation, maintaining a 25° field of view. Ten plants were measured in each plot, and the average reflectance curve was computed to represent each experimental unit.

Figure 5. The Blue Wave spectroradiometer.

The hyperspectral dataset served two complementary purposes:

(1) to radiometrically calibrate and validate the Mavic 3M reflectance values, ensuring physical consistency between aerial and ground measurements;

(2) to be used directly in productivity modeling, along with the UAV multispectral data, for developing multispectral and hyperspectral yield prediction models.

Radiometric calibration was conducted using a Spectralon reference panel (99% reflectance) before and after each acquisition, enabling the conversion of raw digital numbers into hemispherical–conical reflectance factors (Aasen et al., 2018). Throughout data collection, temperature, humidity, and sky conditions were continuously monitored to maintain the temporal stability of spectral responses and reduce measurement drift.

2.4 Processing

Reflectance conversion was performed using a linear empirical model (Equation 1), with coefficients derived from the spectroradiometer data. This method establishes a direct

relationship between UAV digital numbers (DN) and surface reflectance, enhancing spectral comparability across sensors (Martins et al., 2023).

$$Reflectance = a * DN + b \quad (1)$$

where, a represents the coefficient scaling factor.
DN the intensity of the recorded signal.
b represents the calibration offset.

Processing was carried out in Agisoft Metashape Professional 2.1 to generate the orthomosaic, followed by ENVI 5.1 for calibration and spectral extraction. Plot segmentation was based on georeferenced polygons derived from RTK data, ensuring precise alignment between reflectance values and physical plots. Noise filtering and outlier removal were performed using pixel-based statistics in QGIS 3.34.

2.5 Index Calculation

Six vegetation indices were calculated (Equations 02 to 07) for both multispectral and hyperspectral data: Normalized Difference Vegetation Index (NDVI), Green Normalized Difference Vegetation Index (GNDVI), Normalized Difference Vegetation Index (NDRE), Red Edge Normalized Vegetation Index (RENDVI), Chlorophyll Index – Red Edge (CIRE) and Photochemical Reflectance Index (PRI).

These indices are widely used to assess vigor, biomass, and pigment-related stress in perennial crops (Lu et al., 2019; Zhou et al., 2025; Martins et al., 2023).

$$NDVI = \frac{(NIR+R)}{(NIR-R)} \quad (2)$$

$$GNDVI = \frac{(NIR+G)}{(NIR-G)} \quad (3)$$

$$NDRE = \frac{(NIR+RE)}{(NIR-RE)} \quad (4)$$

$$RENDVI = \frac{(RE+R)}{(RE-R)} \quad (5)$$

$$CIRE = \frac{NIR}{RE} - 1 \quad (6)$$

$$PRI = \frac{R_{531} - R_{570}}{R_{531} + R_{570}} \quad (7)$$

where, NIR represent the Near-Infrared band.
R represents the Red band.
G represents the Green band.
RE represents the Red Edge band.
R_{531} represents the Red band at 531 nm.
R_{570} represents the Red band at 570 nm.

2.6 Statistical Analysis and Predictive Modeling

Reflectance values were extracted from both multispectral and hyperspectral datasets. In each plot, measurements were taken from the three central plants to minimize border effects, and the mean reflectance of these plants was used to represent each experimental unit. A total of 39 plots (Fig.1) were analyzed, generating 39 spectral values for each band or index in both multispectral and hyperspectral domains.

Descriptive statistics and Pearson's correlation were applied to identify the most relevant spectral predictors associated with coffee productivity (fresh fruit weight per plot). Only variables showing significant correlation ($p < 0.05$) were used as inputs for predictive modeling. Four regression algorithms were tested to model coffee yield:

- Simple Linear Regression (SLR),
- Multiple Linear Regression (MLR),
- Support Vector Machines (SVM), and
- Artificial Neural Networks (ANN).

All models were implemented in Weka 3.9.6, using the leave-one-out cross-validation (LOOCV) method for model evaluation. This validation approach systematically removes one instance from the dataset for testing while training the model on the remaining samples. The process repeats until every instance has been used once as a test case. LOOCV was chosen because it maximizes the use of limited samples and provides a robust estimation of model generalization performance by minimizing bias and variance.

For Simple Linear Regression (SLR), the default configuration of Weka was used, with a batch size of 100, ridge parameter of 1.0E−8, and two decimal places for output precision. The Multiple Linear Regression (MLR) model employed the M5 attribute selection method, with collinearity elimination enabled and the same ridge correction (1.0E−8) to prevent overfitting.

The Support Vector Machine (SVM) model was implemented through the SMOreg function, using a polynomial kernel (PolyKernel) with exponent = 1.0 and complexity parameter C = 1.0. The optimization algorithm followed the RegSMOImproved configuration with tolerance T = 0.001 and epsilon = 1.0E−12. Data normalization was applied prior to training to ensure stable convergence.

The Artificial Neural Network (ANN) model was based on a feed-forward multilayer perceptron trained with backpropagation. It used a single hidden layer (automatically defined according to the number of inputs), learning rate = 0.3, momentum = 0.2, and training time = 500 epochs, employing the sigmoid activation function. Both input attributes and numeric classes were normalized before training.

Model performance was evaluated using the Relative Root Mean Square Error (RMSE, %) and the Pearson correlation coefficient (R) between observed and predicted productivity values. The overall evaluation aimed to minimize prediction error and identify the most accurate spectral–model combinations for operational monitoring of coffee productivity.

3. Results

Pearson's correlation analysis revealed distinct response patterns between multispectral and hyperspectral datasets (Table 1). In the

multispectral domain, correlation coefficients ranged from -0.56 to 0.70. The Red Edge band showed the strongest positive correlation with coffee productivity ($r = 0.70$, $p < 0.05$), followed by the Green band ($r = 0.64$, $p < 0.05$). The Red band presented a moderate positive relationship ($r = 0.38$, $p < 0.05$). The NDVI index exhibited a negative correlation ($r = -0.56$, $p < 0.05$). Other multispectral indices, such as RENDVI ($r = -0.09$) and CIRE ($r = -0.01$), displayed non-significant relationships with productivity.

For the hyperspectral dataset, correlations were consistently higher and more uniform, ranging from -0.53 to 0.81. The NDRE index achieved the highest correlation with productivity ($r = 0.81$, $p < 0.01$), followed by GNDVI ($r = 0.77$, $p < 0.01$), CIRE ($r = 0.72$, $p < 0.01$), and PRI ($r = 0.55$, $p < 0.01$). The NDVI also presented a significant but negative correlation ($r = -0.53$, $p < 0.01$), while RENDVI showed no significant association ($r = -0.23$).

The range of correlation values among variables indicates that both datasets captured variability related to productivity but with different sensitivities. The hyperspectral data presented higher average correlation coefficients and lower standard deviation among spectral indices, suggesting a more stable relationship between reflectance and fruit weight at this scale.

Spectral Variable	Data Type	Correlation (r)	p-value
Green	Multispectral	0.64	< 0.05
Red	Multispectral	0.38	< 0.05
Red Edge	Multispectral	0.70	< 0.05
NDVI	Multispectral	-0.56	< 0.05
GNDVI	Multispectral	0.38	< 0.05
NDRE	Multispectral	0.40	< 0.05
RENDVI	Multispectral	-0.09	ns
CIRE	Multispectral	-0.01	ns
NDVI	Hyperspectral	-0.53	< 0.01
GNDVI	Hyperspectral	0.77	< 0.01
NDRE	Hyperspectral	0.81	< 0.01
RENDVI	Hyperspectral	-0.23	ns
CIRE	Hyperspectral	0.72	< 0.01
PRI	Hyperspectral	0.55	< 0.01

Table 1. Pearson correlation between spectral variables and coffee productivity (ns: non significative).

Prediction models based on multispectral data achieved satisfactory performance, with variable accuracy across the tested algorithms (Table 2). Within the multispectral group, the Artificial Neural Network (ANN) achieved the best predictive performance, with RMSE = 12.1% and R = 0.88, followed by the Support Vector Machine (SVM), which reached RMSE = 13.5% and R = 0.84. The Multiple Linear Regression (MLR) model presented intermediate accuracy (RMSE = 19.7%, R = 0.71), while Simple Linear Regression (SLR) recorded the lowest performance (RMSE = 23.1%, R = 0.65).

In contrast, models derived from hyperspectral data showed consistently higher correlation coefficients and lower RMSE values than those from multispectral data. The ANN model achieved the highest accuracy overall (RMSE = 7.9%, R = 0.93), followed by SVM (RMSE = 9.2%, R = 0.90). The MLR model obtained intermediate results (RMSE = 14.8%, R = 0.81), and SLR reached RMSE = 18.9% with R = 0.74.

Model	Data Type	RMSE (%)	R
SLR	Multispectral	23.1	0.65
MLR	Multispectral	19.7	0.71
SVM	Multispectral	13.5	0.84
ANN	Multispectral	12.1	0.88
SLR	Hyperspectral	18.9	0.74
MLR	Hyperspectral	14.8	0.81
SVM	Hyperspectral	9.2	0.90
ANN	Hyperspectral	7.9	0.93

Table 2. Performance of predictive models using multispectral and hyperspectral data.

Residual dispersion analysis confirmed the presence of lower variability in hyperspectral model outputs, with smaller prediction errors and tighter agreement between observed and predicted productivity values. Across all tested algorithms, the reduction in RMSE was proportional to the increase in spectral resolution and model complexity.

Overall, numerical comparisons indicate that predictive performance improved progressively from linear to nonlinear models and from multispectral to hyperspectral data. The difference between ANN and SVM results was less pronounced for hyperspectral inputs, suggesting a convergence in performance at higher spectral detail levels. The hierarchy among models remained stable across datasets, with neural networks consistently achieving the lowest RMSE and the highest correlation with observed productivity values.

4. Discussion

The results demonstrated clear distinctions between multispectral and hyperspectral datasets in predicting coffee productivity, reflecting the influence of spectral resolution and information depth on model performance. The higher correlations and lower prediction errors obtained with hyperspectral data confirm its enhanced capability to capture subtle canopy variations that are often diluted in broadband multispectral imagery. Similar findings have been reported in perennial crops, where hyperspectral reflectance provided better discrimination of biochemical and structural traits associated with yield (Joshi et al., 2023; Khan et al., 2022).

In coffee, differences in reflectance behavior are strongly related to canopy composition and phenological stage. During the fruiting period, photosynthates are redirected from vegetative tissues to fruit filling, resulting in lower near-infrared (NIR) reflectance and reduced NDVI values in highly productive plants. This inverse relationship between vegetative vigor and yield is well-documented for Coffea arabica and other woody crops (Martins et al., 2023). Consequently, indices such as NDVI may not represent productivity directly but instead indicate canopy development, which tends to stabilize or decline in mature, fruit-bearing plants.

The positive correlations observed for the Red Edge and Green bands in the multispectral dataset indicate sensitivity to chlorophyll concentration and canopy pigment status. The Red Edge region, in particular, is widely recognized as a reliable proxy for leaf biochemical composition, responding linearly to chlorophyll variation even in dense canopies (Clevers & Gitelson, 2013; Xue & Su, 2017). The Green band, though broader, captures reflectance peaks associated with photosynthetically active tissues, reinforcing its relevance in identifying areas of high physiological activity. The PRI index

also showed good association with productivity, highlighting its responsiveness to changes in xanthophyll cycle pigments and light-use efficiency, as reported in previous studies (Garbulsky et al., 2011; Radočaj et al., 2023).

In hyperspectral data, the NDRE, GNDVI, CIRE, and PRI indices exhibited the strongest relationships with coffee yield. These indices operate within narrow spectral ranges that correspond to pigment absorption features and canopy stress indicators. The NDRE leverages the sensitivity of the red-edge transition to chlorophyll and nitrogen dynamics, whereas GNDVI emphasizes variations in photosynthetic capacity linked to canopy density. The CIRE index, based on the NIR-to-Red Edge ratio, has been shown to be particularly effective in quantifying chlorophyll concentration and early stress detection in perennial crops (Sahoo et al., 2024; Singh, et al., 2020). The PRI, in particular, reflects variations in the xanthophyll pigment cycle and photosynthetic efficiency, providing information on light-use dynamics and stress response (Garbulsky et al., 2011). These indices operate within narrow spectral ranges that correspond to pigment absorption features and canopy stress indicators. Together, they confirm that hyperspectral narrowband indices provide more accurate indicators of physiological traits directly associated with yield potential. Together, these results confirm that hyperspectral narrowband indices provide more accurate indicators of physiological traits directly associated with yield potential.

Model performance followed a clear trend across data types and algorithm complexity. Neural networks and support vector machines achieved the best predictive accuracy for both multispectral and hyperspectral inputs. These models are particularly suited for nonlinear relationships and high-dimensional datasets, where interactions between spectral variables are complex and not easily captured by linear regressions (Upadhyay et al., 2025; Wang et al., 2024). The ability of ANN models to generalize from limited samples is a crucial advantage for precision agriculture studies, where data collection is often constrained by logistical and temporal limitations.

The improvement in predictive accuracy from multispectral to hyperspectral inputs highlights the trade-off between operational simplicity and spectral precision. While hyperspectral data provide superior quantitative information, their acquisition is more demanding, requiring calibration standards, controlled lighting, and stable measurement geometry. In contrast, UAV multispectral sensors are more practical and allow coverage of larger areas at lower cost and faster turnaround, making them suitable for operational monitoring in commercial coffee production systems (Aasen et al., 2018; Martins et al., 2023). The present results suggest that both approaches can be complementary: hyperspectral data may serve as a calibration reference for developing robust multispectral models applicable at scale.

The integration of multiscale spectral data and machine learning thus represents a powerful framework for precision phenotyping in coffee crops. By aligning ground-based hyperspectral precision with aerial multispectral coverage, it is possible to balance detail and scalability, enabling both experimental research and applied management. Moreover, the use of AI-based models expands the analytical capability beyond simple correlations, enabling yield estimation under heterogeneous conditions that characterize perennial crops. This approach can be extended to temporal analyses, combining seasonal image series to monitor canopy development and forecast yield across harvest cycles.

Finally, the results obtained here provide a methodological foundation for further studies aiming to refine yield prediction in coffee and other high-value perennial crops. Future research may explore feature selection techniques, hybrid spectral–structural variables, and multi-temporal modeling to improve robustness. Integration with additional data sources, such as LiDAR or thermal imagery, could further enhance the understanding of crop physiology and productivity at different spatial scales.

5. Future Perspectives, Advantages, and Limitations

The hyper–multispectral approach proved highly feasible for estimating coffee yield by combining the spectral precision of hyperspectral field data with the spatial coverage of UAV-based multispectral imagery. This integration minimizes radiometric uncertainty through cross-calibration and enables the creation of operational predictive models, particularly when coupled with artificial intelligence algorithms such as ANN and SVM. The main contribution of this study lies in the acquisition and calibration protocol, which includes the use of reference panels, RTK positioning, solar window control, and empirical correction. These procedures ensure data comparability across sensors and scales, providing a reproducible framework for large-scale monitoring.

The present experiment, however, was conducted on a single canopy within a single plot. While this setting allowed for controlled conditions and precise calibration, it limits the generalization of results to commercial plantations that exhibit substantial heterogeneity. In real production areas, factors such as irrigation versus rainfed management, pruning systems, fertilization regimes, and row spacing all influence canopy structure and spectral response, potentially changing which indices best correlate with yield. Additionally, coffee’s biennial cycle and its distinct phenological stages—flowering, pinhead fruit, expansion, and maturation—alter canopy vigor, pigment concentration, and structure. These variations can even reverse the expected relationships between spectral indices and productivity, as highly productive plants often show lower NDVI during harvest due to assimilate allocation to fruits.

Field yield measurements themselves also lack standardization, whether recorded as fresh weight per plant, per plot, or by volumetric or subsampled estimates, which further complicates the comparison between studies. Future improvements should include expanding experiments to multiple commercial fields with cross-site validation across different cultivars and management systems. Multitemporal campaigns spanning at least two years are recommended to capture biennial variability and train phenology-sensitive models. It is also essential to standardize acquisition protocols such as flight altitude and speed, solar time, spectroradiometer height and field of view, use of reference panels, and documentation of environmental metadata, along with detailed operational checklists to ensure reproducibility.

Harmonizing sensors through radiometric transfer functions, using empirical DN-to-reflectance curves and post-flight validation with 10%, 50%, and 99% panels, is crucial to reduce the black-box effect of internal corrections in UAV systems like the Mavic 3M. Analytical improvements should focus on developing phenology-aware or mixed-effects models that account for plot-level variability, feature selection and engineering (including narrowband regions, red-edge position,

and pigment indices), and model interpretability tools such as SHAP to enhance transparency. Incorporating uncertainty quantification, domain transfer techniques to adapt models between farms, and ensemble or regularized algorithms can further improve model robustness and scalability.

Integration with other remote sensing modalities such as thermal (water status), LiDAR (canopy structure), and multisensor time series like Sentinel-2 for phenological tracking could enhance prediction and enable pre-harvest yield estimation during flowering or fruit filling. For operational implementation, the development of a minimal index set and a rapid in-field recalibration routine with anchor samples and reflectance panels is advisable. In this framework, hyperspectral data serve as a calibration reference, while multispectral data act as a scalable monitoring tool for precision agriculture applications.

6. Conclusion

Hyperspectral data, despite greater acquisition complexity, achieved superior results in coffee productivity prediction, particularly when integrated into artificial neural network models. This performance reflects the high spectral resolution and the ability of hyperspectral sensing to capture subtle physiological variations related to pigment concentration, canopy structure, and stress dynamics in perennial crops. Within the multispectral dataset, the Red Edge and Green bands demonstrated notable sensitivity to productivity patterns, while the Photochemical Reflectance Index (PRI), derived from hyperspectral measurements, also yielded significant results in support vector machine (SVM) models.

The adopted multiscale approach highlights the complementary potential of both data sources. While hyperspectral data enable more detailed biophysical characterization, multispectral imagery represents a practical and cost-effective alternative for operational monitoring, providing satisfactory accuracy levels in yield prediction tasks. These findings reinforce the feasibility of using multispectral sensors in large-scale precision agriculture programs, particularly when combined with robust machine learning algorithms.

Overall, the results indicate that integrating remote sensing and data-driven modeling contributes to advancing precision phenotyping techniques for coffee crops. The methodological framework developed in this study can support future research focusing on temporal analysis, environmental variability, and the adaptation of predictive models to different cultivars and growth stages. Moreover, it establishes a foundation for developing operational monitoring systems capable of assisting management decisions, resource optimization, and yield forecasting in sustainable coffee production systems.

Acknowledgements

The authors thank the Coordination for the Improvement of Higher Education Personnel (CAPES) for funding master's scholarships that supported the development of this research: to authors Lucas Henrique Vicentini Viana de Carvalho (Process 88887.000652/2024-00), Filipe Vieira da Silva (Process 88887.951609/2024-00) and Maria Cecília Lemes Santos (Process 88887.138846/2025-00).

References

AASEN, H. et al. (2018). Quantitative remote sensing at ultra-high resolution with UAV spectroscopy: A review of sensor technology, measurement procedures, and data correction workflows. *Remote Sensing*, v. 10, n. 7, p. 1091. https://doi.org/10.3390/rs10071091

Clevers, J. G. P. W., & Gitelson, A. A. (2013). Remote estimation of crop and grass chlorophyll and nitrogen content using red-edge bands on Sentinel-2 and -3. *International Journal of Applied Earth Observation and Geoinformation*, 23, 344–351. https://doi.org/10.1016/j.jag.2012.10.008.

FAO. Coffee Market Report 2024. Rome: Food and Agriculture Organization of the United Nations, 2024.

Garbulsky, M. F. et al. (2011). The photochemical reflectance index (PRI) and the remote sensing of leaf, canopy and ecosystem radiation use efficiencies: A review and meta-analysis. *Remote sensing of environment*, v. 115, n. 2, p. 281-297. https://doi.org/10.1016/j.rse.2010.08.023.

ICO. Coffee Development Report 2023. London: International Coffee Organization, 2023.

Joshi, A. et al. (2023). Remote-sensing data and deep-learning techniques in crop mapping and yield prediction: A systematic review. *Remote Sensing*, v. 15, n. 8, p. 2014. https://doi.org/10.3390/rs15082014.

Khan, A. et al. (2022). A systematic review on hyperspectral imaging technology with a machine and deep learning methodology for agricultural applications. *Ecological Informatics*, v. 69, p. 101678. https://doi.org/10.1016/j.ecoinf.2022.101678.

Lu, B. et al. (2019). Comparing the performance of multispectral and hyperspectral images for estimating vegetation properties. *IEEE Journal of selected topics in applied earth observations and remote sensing*, v. 12, n. 6, p. 1784-1797. DOI: 10.1109/JSTARS.2019.2910558.

Martins, R. N. et al. (2023) Digital mapping of coffee ripeness using UAV-based multispectral imagery. *Computers and Electronics in Agriculture*, v. 204, p. 107499. https://doi.org/10.1016/j.compag.2022.107499.

Radočaj, D. et al. (2023). State of major vegetation indices in precision agriculture studies indexed in web of science: A review. *Agriculture*, v. 13, n. 3, p. 707. https://doi.org/10.3390/agriculture13030707.

Rosas, J. T. F. et al. (2022). Coffee ripeness monitoring using a UAV-mounted low-cost multispectral camera. *Precision Agriculture*, v. 23, n. 1, p. 300-318. https://doi.org/10.1007/s11119-021-09838-3.

Sahoo, R. N. et al. (2024). Estimation of wheat biophysical variables through UAV hyperspectral remote sensing using machine learning and radiative transfer models. *Computers and Electronics in Agriculture*, v. 221, p. 108942, 2024. https://doi.org/10.1016/j.compag.2024.108942.

Singh, P. et al. (2020). Hyperspectral remote sensing in precision agriculture: Present status, challenges, and future trends. In: *Hyperspectral remote sensing*. *Elsevier*. p. 121-146. https://doi.org/10.1016/B978-0-08-102894-0.00009-7.

Sun, H. et al. (2022). Crop Sensing in Precision Agriculture. In: Soil and Crop Sensing for Precision Crop Production. Cham:

Springer International Publishing. p. 251-293. https://doi.org/10.1007/978-3-030-70432-2_8.

Upadhyay, A. et al. (2025). Deep learning and computer vision in plant disease detection: a comprehensive review of techniques, models, and trends in precision agriculture. *Artificial Intelligence Review*, v. 58, n. 3, p. 92. https://doi.org/10.1007/s10462-024-11100-x.

Wang, J. et al. (2024). Integration of remote sensing and machine learning for precision agriculture: a comprehensive perspective on applications. *Agronomy*, v. 14, n. 9, p. 2024. https://doi.org/10.3390/agronomy14091975.

Xue, J., & Su, B. (2017). Significant remote sensing vegetation indices: A review of developments and applications. *Journal of Sensors*, 2017, 1353691. https://doi.org/10.1155/2017/1353691.

Zhou, H. et al. (2025). Yield prediction through UAV-based multispectral imaging and deep learning in rice breeding trials. *Agricultural Systems*, v. 223, p. 104214. https://doi.org/10.1016/j.agsy.2024.104214.